Chemistry & Biology
Article

Interplay between the Ribosomal Tunnel, Nascent Chain, and Macrolides Influences Drug Inhibition

Agata L. Starosta,[1,2] Viktoriya V. Karpenko,[3] Anna V. Shishkina,[4] Aleksandra Mikolajka,[1,2] Natalia V. Sumbatyan,[3] Frank Schluenzen,[5] Galina A. Korshunova,[4] Alexey A. Bogdanov,[3,4,*] and Daniel N. Wilson[1,2,*]
[1]Gene Center and Department of Biochemistry
[2]Center for Integrated Protein Science Munich
University of Munich, LMU, Munich D-81377, Germany
[3]Department of Chemistry
[4]A.N. Belozersky Institute of Physico-Chemical Biology,
M.V. Lomonosov Moscow State University, Moscow 119992, Russia
[5]Deutsches Elektronen-Synchrotron, Hamburg D-22603, Germany
*Correspondence: bogdanov@genebee.msu.su (A.A.B.), wilson@lmb.uni-muenchen.de (D.N.W.)
DOI 10.1016/j.chembiol.2010.04.008

SUMMARY

Accumulating evidence suggests that, during translation, nascent chains can form specific interactions with ribosomal exit tunnel to regulate translation and promote initial folding events. The clinically important macrolide antibiotics bind within the exit tunnel and inhibit translation by preventing progression of the nascent chain and inducing peptidyl-tRNA drop-off. Here, we have synthesized amino acid– and peptide-containing macrolides, which are used to demonstrate that distinct amino acids and peptides can establish interaction with components of the ribosomal tunnel and enhance the ribosome-binding and inhibitory properties of the macrolide drugs, consistent with the concept that the exit tunnel is not simply a Teflon-like channel. Surprisingly, we find that macrolide antibiotics do not inhibit translation of all nascent chains similarly, but rather exhibit polypeptide-specific inhibitory effects, providing a change to our general mechanistic understanding of macrolide inhibition.

INTRODUCTION

The translational machinery represents one of the major targets within the cell for antibiotics (reviewed by Spahn and Prescott, 1996; Wilson, 2009). The majority of antibiotics inhibit protein synthesis by binding at the active centers on the ribosome; for example, the tetracyclines and aminoglycosides (gentamicin) bind within the decoding site on the small subunit, whereas the phenylpropanoids (chloramphenicol) and oxazolidinones (linezolid) bind within the A-site of peptidyltransferase center (PTC) to block peptide-bond formation. In contrast, the clinically important class of macrolide antibiotics bind within the ribosomal exit tunnel, where they are thought to inhibit translation by blocking elongation of the nascent polypeptide chain, which, in turn, induces peptidyl-tRNA drop-off (Mankin, 2008; Poehlsgaard and Douthwaite, 2003).

Macrolides are a diverse family of antibiotics that contain a central 12–16-membered lactone ring to which various sugar substituent's are attached; for example, erythromycin has a 14-membered ring with C3 cladinose and C5 desosamine sugars (Figure 1), whereas tylosin has a 16-membered ring with a C5 mycaminose-mycarose disaccharide as well as a C23 mycinose (Figures 1 and 2). Crystal structures of macrolides bound to the large ribosomal subunit reveal that the drugs bind within the ribosomal exit tunnel adjacent to the peptidyltransferase center (Figures 2A and 2B) (Hansen et al., 2002; Schlünzen et al., 2001). Surprisingly, 16-membered macrolides that have a C6 ethyl aldehyde (with the aldehyde functional group at C20), such as tylosin (Figure 1), form a reversible covalent bond with the N6 of adenine 2062 (A2062; *Escherichia coli* numbering used throughout) of the 23S ribosomal RNA (Figure 2B) (Hansen et al., 2002). The lactone rings of different macrolides are generally positioned in the tunnel with very similar orientations, such that the C5 sugars extend up the tunnel toward the PTC (Hansen et al., 2002; Poulsen et al., 2000; Schlünzen et al., 2001; Wilson et al., 2005) (Figure 2B). Consistently, macrolides such as erythromycin with only a single C5 sugar allow synthesis of short oligopeptides of six to eight amino acids before peptidyl-tRNA drop-off occurs, whereas macrolides with C5 disaccharides, such as tylosin, allow only two to four amino acids to be synthesized (Tenson et al., 2003), and can even directly inhibit the peptidyltransferase reaction (Karahalios et al., 2006).

It should be noted, however, that the length of the peptide synthesized before peptidyl-tRNA drop-off appears to be dependent on the sequence being translated (Tenson et al., 2003). Translation of short nascent pentapeptides of defined sequence can lead to dissociation of macrolide antibiotics from the ribosome and thus confer macrolide resistance (Lovmar et al., 2006; Tenson et al., 1996; Tenson and Mankin, 2001). Moreover, different pentapeptide sequences can confer resistance to distinct macrolide members, suggesting a direct and discriminating interaction between the nascent chain and the

 ©2010 Elsevier Ltd All rights reserved

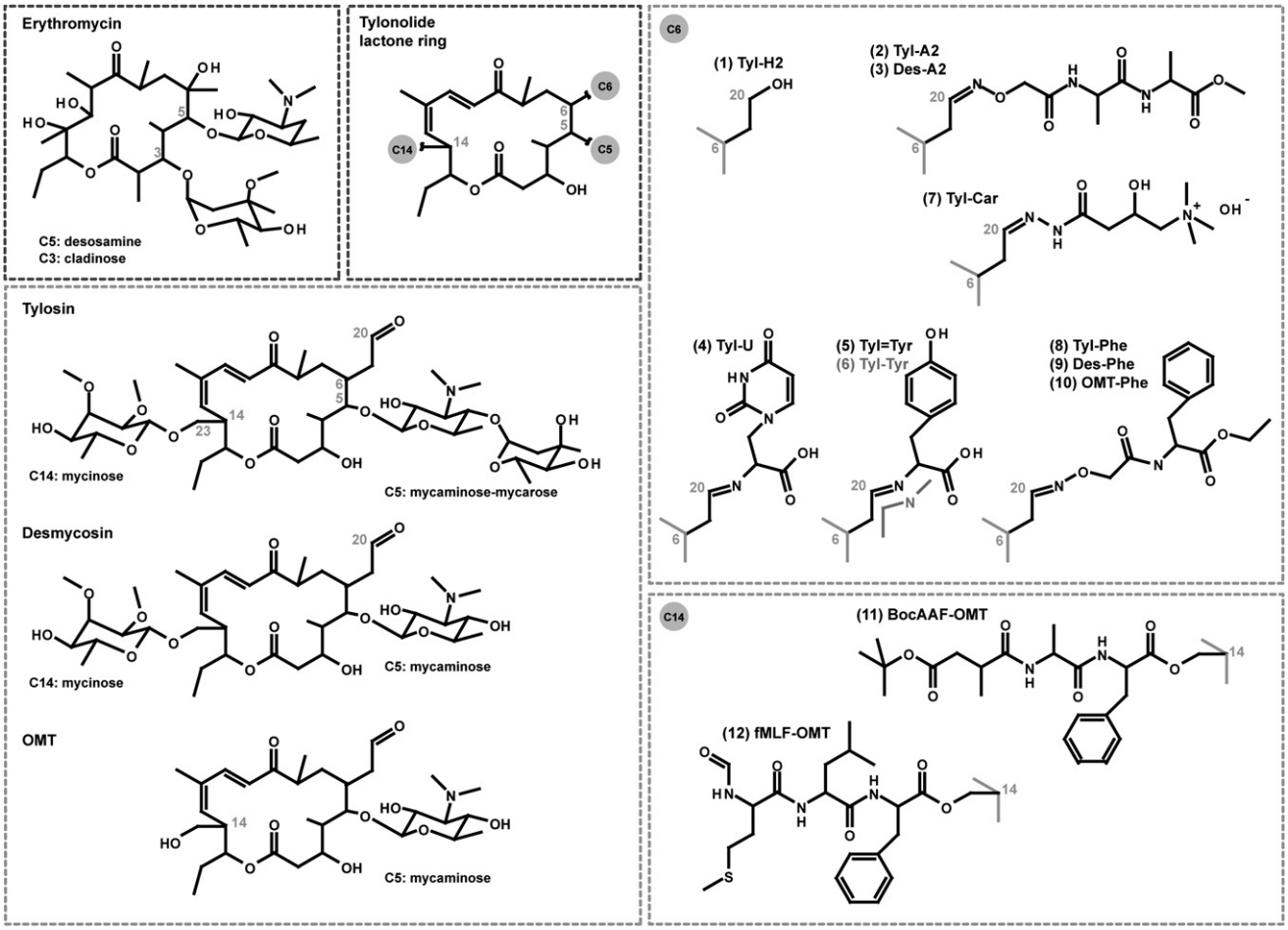

Figure 1. Chemical Structures of Macrolide Antibiotics

Chemical structures of tylosin (Tyl), desmycosin (Des), OMT, erythromycin, and derivatives used in this study (**1**)–(**12**) are depicted.

macrolide (Tenson et al., 1997; Tripathi et al., 1998; Vimberg et al., 2004). Inducible expression of some macrolide resistance genes, such as the methyltransferase encoded by the *ermC* gene, requires macrolide-dependent translational stalling during the synthesis of an upstream leader peptide (Mayford and Weisblum, 1989; Ramu et al., 2009; Vazquez-Laslop et al., 2008). Mutations in the ErmC leader peptide as well as within components of the ribosomal exit tunnel, namely A2062 of the 23S rRNA, have been identified that relieve the translational stalling (Ramu et al., 2009; Vazquez-Laslop et al., 2008), suggesting

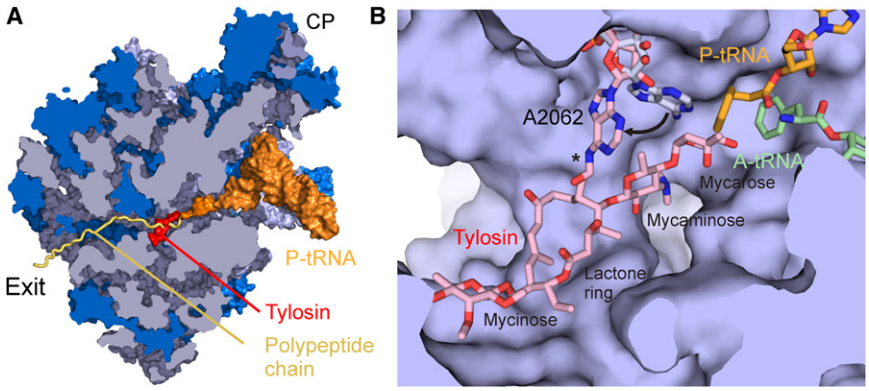

Figure 2. Binding of Macrolide Antibiotics Within the Ribosomal Tunnel

(A) Transverse section through the large subunit of the ribosome to visualize the ribosomal exit tunnel. The position of tylosin (red), P-site tRNA (orange), and a mock polypeptide chain (yellow) are indicated. CP, central protuberance; rRNA, gray and ribosomal proteins (dark blue).

(B) Zoom in on the macrolide-binding site within the ribosomal tunnel. Tylosin (pink) shown with lactone ring, C23-mycinose, and C5-mycaminose-mycarose are labeled. The asterisk indicates the carbinolamine bond that forms between tylosin and the N6 of 23S rRNA nucleotide A2062, whereas the arrow indicates the shift in A2062 seen upon ligand binding. The positions of A- and P-site aminoacyl-tRNAs are shown in green and orange, respectively.

a complex interplay between the antibiotic, the tunnel, and the nascent polypeptide chain.

Although the ribosomal tunnel has for many years been thought of as a passive conduit for the nascent chain, accumulating evidence indicates the existence of many specific leader peptides that induce translational stalling by directly interacting with the ribosomal tunnel, and in doing so regulate translation of a downstream gene (Tenson and Ehrenberg, 2002). Indeed, recent cryo-EM reconstructions directly visualize interaction between the nascent polypeptide chain and components of the ribosomal tunnel (Becker et al., 2009; Bhushan et al., 2010; Seidelt et al., 2009). Moreover, interaction between the nascent chain and tunnel has been proposed to play a more general role in modulating translation rate (Lu and Deutsch, 2008; Seidelt et al., 2009) as well as influencing initial protein folding events (Bhushan et al., 2010; Kosolapov and Deutsch, 2009; Lu and Deutsch, 2005a, 2005b; Woolhead et al., 2004).

Here, we demonstrate that abolishing the potential of tylosin to form a covalent bond with A2062 of the ribosome dramatically reduces the binding and inhibitory properties of the drug, but that this can be reversed by the addition of amino acid and peptide side chains that enable interaction to be reestablished with the ribosomal exit tunnel. A number of the macrolide-peptide compounds are even more potent inhibitors of translation than their parent compounds. Surprisingly, we find that macrolides exhibit nascent chain-specific effects: 5-O-mycaminosyl-tylonolid (OMT), a precursor of tylosin, has excellent antimicrobial activity and is a potent inhibitor of firefly luciferase synthesis. In contrast, OMT is a very poor inhibitor of green fluorescent protein synthesis and can even protect the translational apparatus from the inhibitory effects of other macrolides, such as erythromycin and tylosin. Differential effects are also observed for other macrolide antibiotics but are not seen for non-macrolide antibiotics, such as tetracyclines and chloramphenicols. Collectively, our results demonstrate the direct and specific interaction between peptides and the ribosomal tunnel and suggest that the inhibitory effect of macrolides is dependent on the sequence of the nascent polypeptide chain being translated.

RESULTS

Peptide Interaction with the Tunnel Compensates for Loss of the Covalent Bond

To investigate the effect of the covalent linkage between the C6 ethyl aldehyde of tylosin and the N6 of A2062 of the 23S rRNA (Figure 2B), we synthesized a reduced form of tylosin, (**1**) Tyl-H2, where the C6 ethyl aldehyde is replaced by hydroxyethyl group (Figure 1A). Binding of (**1**) Tyl-H2 to the ribosome was monitored by competition with radiolabeled [^{14}C]-erythromycin (apparent K_d calculations in Table S1, available online, are based on a 2 hr incubation; see Experimental Procedures). In the control experiment, we demonstrate that tylosin is an excellent competitor, completely abolishing the binding of erythromycin at ~0.1 μM (Figure 3A). In contrast, (**1**) Tyl-H2 was totally inactive, and no significant loss in erythromycin binding was observed with 100× higher concentrations (10 μM) of the compound (Figure 3A). These results support the importance of the carbinolamine covalent linkage for efficient ribosome binding, in agreement with previous findings that modification of the C20 aldehyde group leads to a ~100-fold increase in the MIC value for a variety of gram-positive bacteria (Kirst et al., 1988; Narandja et al., 1994; Omura et al., 1982; Omura and Tishler, 1972).

Next, we synthesized a series of macrolide derivatives where amino acids and peptides were attached to the C20 aldehyde position to investigate whether amino acids can establish defined interactions with the ribosomal exit tunnel. We reasoned that if this is indeed the case, then the peptide-tunnel interactions should improve the binding affinity of the compounds. As can be seen in Figure 3A, the presence of Ala-Ala at the C20 position to generate (**2**) Tyl-A2 dramatically improves the ability of the compound to compete with erythromycin for ribosome binding. Similar results were also obtained when Ala-Ala was attached to the C20 position of desmycosin, a degradation product of tylosin differing by the absence of a C5 mycarose, to generate (**3**) Des-A2 (Figure 3A). This finding suggests that, indeed, the Ala-Ala peptides establish interaction with the tunnel to improve the binding of the compounds compared with the Tyl-H2; however, it should be noted that the K_d of (**2**) Tyl-A2 and (**3**) Des-A2 (~18 nM for both compounds) are still significantly worse than their C6 ethyl aldehyde–containing parent compounds tylosin (0.65 nM) and desmycosin (0.3 nM) (Table S1; Figure 3A).

To test the inhibitory activity of the compounds, we utilized an *E. coli* lysate–based, in vitro, coupled transcription-translation system (Dinos et al., 2004; Starosta et al., 2009), where the synthesis of green fluorescent protein (GFP) was monitored by directly measuring fluorescence (Figure 3B). Consistent with the ribosome binding results, tylosin was found to be an excellent inhibitor, with an IC_{50} of 0.25 μM and abolishing translation at ~1 μM (Figures 3B and 3C), whereas (**1**) Tyl-H2 had an IC_{50} > 10× higher (4 μM) (Table S1) and did not even completely abolish translation at 25 μM (data not shown). (**2**) Tyl-A2 exhibited improved inhibitory characteristics, with an IC_{50} of 0.5 μM—only slightly worse than that of tylosin (Figure 3C; Table S1). This contrasts with the binding assay results where (**2**) Tyl-A2 was a significantly worse competitor of erythromycin than tylosin for ribosome binding (Figure 3A). A similar trend was observed when comparing desmycosin with (**3**) Des-A2, in that (**3**) Des-A2 was a slightly more effective inhibitor than desmycosin. However, unlike (**2**) Tyl-A2, both desmycosin and (**3**) Des-A2 could not fully abolish translation even at high concentrations (Figure 3C; Table S1).

We have previously determined a crystal structure of (**2**) Tyl-A2 bound to the *Deinococcus radiodurans* large ribosomal subunit (Wilson et al., 2005), which shows that the lactone ring binds in a similar position to that seen for tylosin (Hansen et al., 2002). The C20 Ala-Ala peptide protrudes into a small alcove or pocket within the tunnel wall, where it stacks against the base of A2062 (Figure 3E). The presence of the C20 Ala-Ala peptide on (**2**) Tyl-A2 precludes formation of the carbinolamine bond with the N6 of A2062, and as a result A2062 is in a shifted position compared to the tylosin-50S structure (Hansen et al., 2002) (Figure 3D).

Optimized Stacking Interactions with A2062 Improves Inhibition

On the basis of the structure of the (**2**) Tyl-A2 bound to the large subunit, a series of novel C6 tylosin derivatives were synthesized that can potentially form better stacking interactions with the

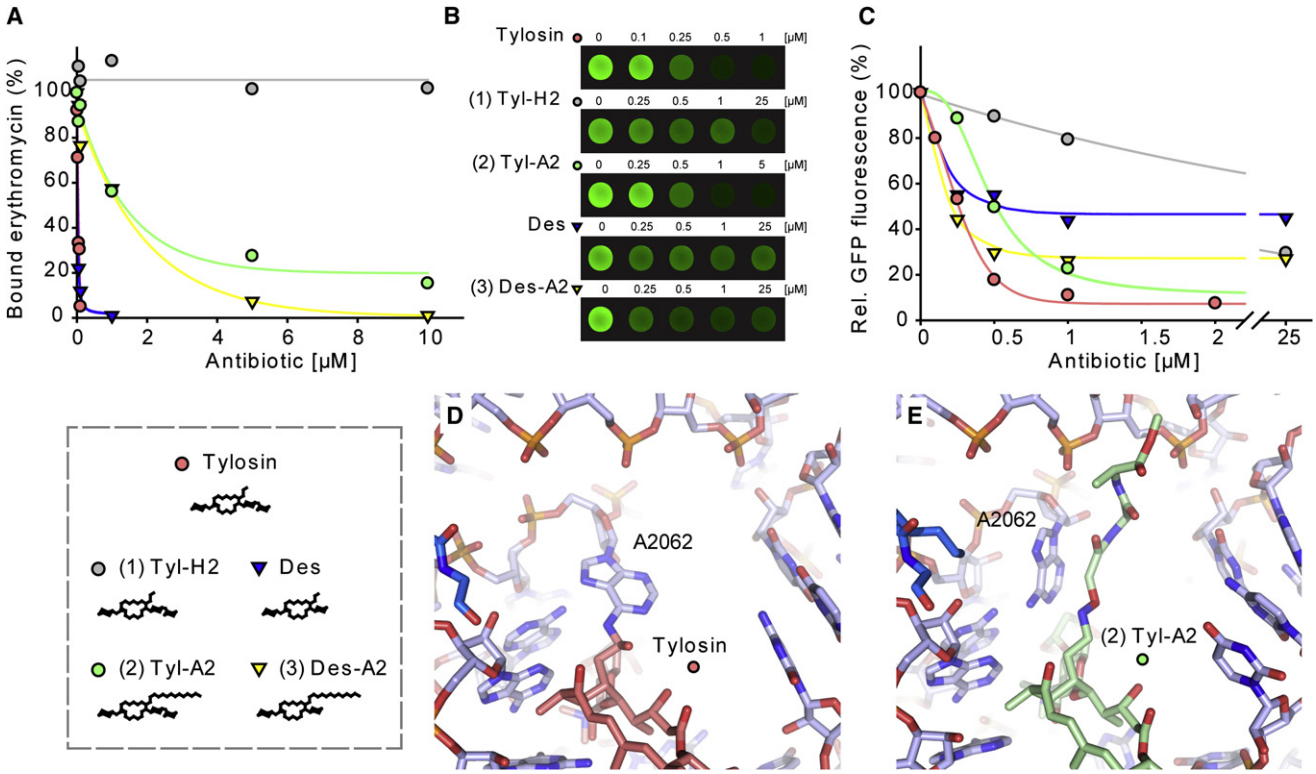

Figure 3. Inhibitory Effect of Tylosin and Desmycosin Ala2 Derivatives

(A) The ability of tylosin (pink), Tyl-H2 (gray), desmycosin (Des, blue), (**2**) Tyl-A2, and (**3**) Des-A2 to compete with radiolabeled erythromycin for binding to *E. coli* 70S ribosomes was determined. The binding of erythromycin in the absence of competing ligand was assigned as 100%.

(B) The amount of GFP produced in an *E. coli* in vitro transcription-translation assay in the presence or absence of tylosin, (**1**) Tyl-H2 and (**2**) Tyl-A2, Des, and (**3**) Des-A2 was determined by monitoring fluorescence of GFP. The fluorescence of GFP in the absence of antibiotic was assigned as 100%.

(C) Quantification of (B) with symbols and colors for each compound as in (A).

(D) The binding site of tylosin on the *H. marismortui* 50S subunit showing the formation of a covalent carbinolamine bond between the C6 ethyl-aldehyde of tylosin (red) and the N6 of the base of A2062 of the 23S rRNA (Hansen et al., 2002).

(E) The binding site of (**2**) Tyl-A2 (green) on the *D. radiodurans* 50S subunit showing the stacking interaction between the Ala-Ala side chain of (**2**) Tyl-A2 and the base of A2062 of the 23S rRNA (Wilson et al., 2005).

base of A2062, namely by introducing aromatic or heterocyclic groups that replace the Ala amino acids. Because base-stacking between RNA nucleotides is an efficient and highly ubiquitous interaction mode within RNA particles, the first compound, (**4**) Tyl-U, was designed with an uridine (U) RNA nucleobase linked to the lactone C6 carbon by a four-atom linker (Figure 1). In the translation assay, (**4**) Tyl-U was still a worse inhibitor than (**2**) Tyl-A2, but was superior to (**1**) Tyl-H2 (Figure 4A; Table S1).

In parallel, we investigated the effect of replacing the Ala-Ala peptide with the amino acid tyrosine (Tyr) to generate the (**5**) Tyl=Tyr derivative, which also utilizes a five-atom linker. Although this compound had improved binding and inhibitory activity with respect to (**1**) Tyl-H2, it was still significantly worse than (**2**) Tyl-A2 (Figures 4A and 4B; Table S1). We rationalized that the double bond in the linker may restrict the conformational freedom of the side chain and therefore synthesized a second compound (**6**) Tyl-Tyr with a fully saturated linker. In the translation assays, (**6**) Tyl-Tyr was a significantly better inhibitor than (**5**) Tyl=Tyr and (**2**) Tyl-A2 (Figure 4B; Table S1), which was consistent with the improved binding properties of (**6**) Tyl-Tyr (Figure 4A). What was curious was (**6**) Tyl-Tyr had an IC_{50} comparable to that of tylosin (Figure 4B; Table S1), despite being less effective than tylosin at competing for ribosome binding with erythromycin (Figure 3A).

In a separate approach, we also attached carnitine to the C20 position to generate (**7**) Tyl-Car (Figure 1). The positively charged side chain improves the aqueous solubility, compared with tylosin, but was also intended to improve interactions with the highly electronegative cleft in the ribosomal tunnel. Indeed, (**7**) Tyl-Car displayed binding (K_d, 0.6 nM) and inhibition (IC_{50}, 0.3) properties very similar to those of tylosin (Figures 4A and 4B; Table S1), suggesting that, like (**2**) Tyl-A2, the side chain of (**7**) Tyl-Car establishes interaction with the ribosomal tunnel that compensate for the loss of the carbinolamine bond. (**7**) Tyl-Car was modeled in the tunnel with the constraint that the lactone ring and A2062 were positioned as in (**2**) Tyl-A2 structure (Wilson et al., 2005). The most energetically favorable solution indicated that the carnitine side chain adopted a conformation that establishes stacking interactions with A2062 (Figure 4C).

Enhanced Tylosin Antibiotics That Utilize Peptide-Tunnel Interaction

To further explore the stacking potential of the C20 side chains with the nucleobase of A2062, we decided to introduce

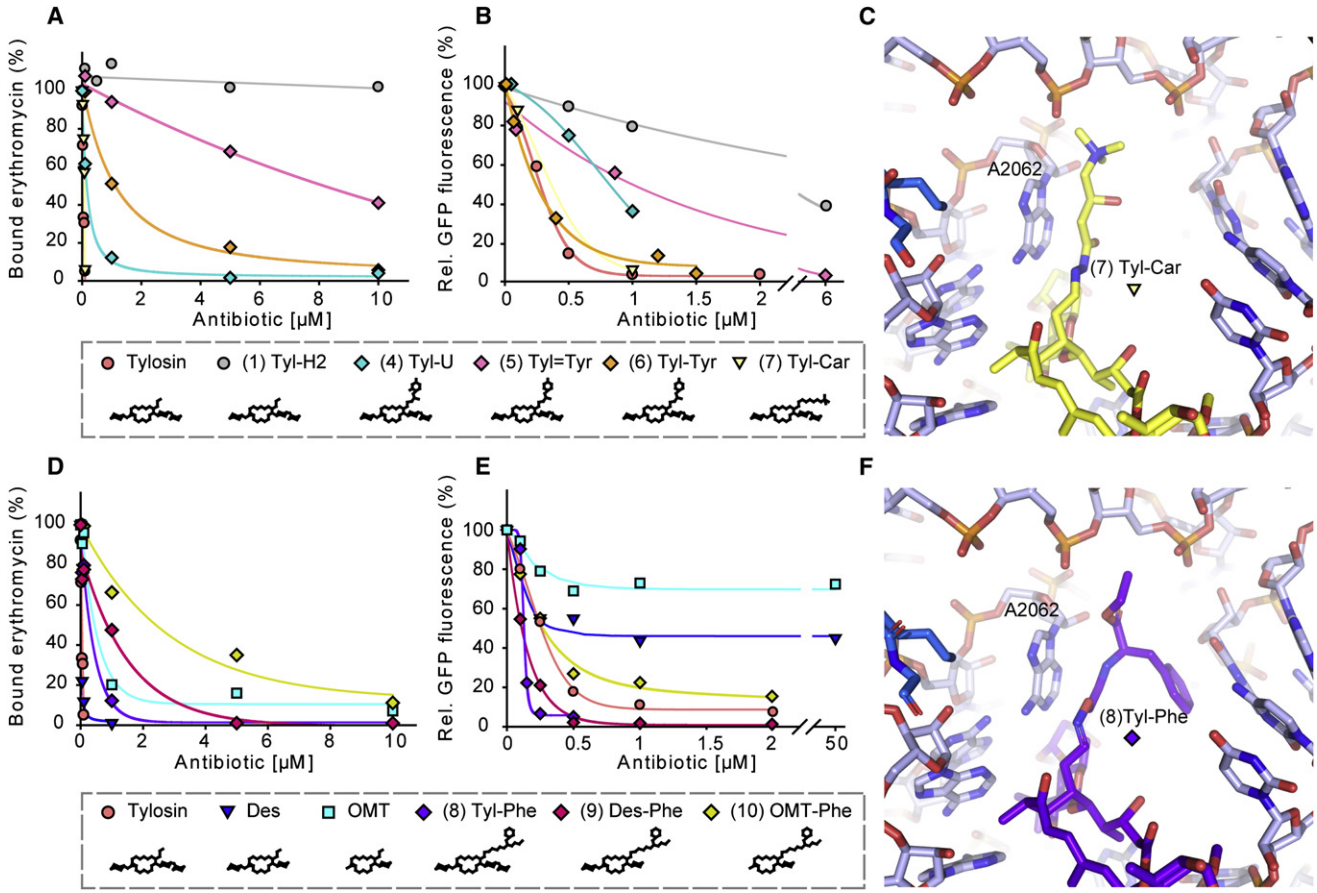

Figure 4. Stacking Interaction with A2062

(A) The ability of tylosin, (**1**) Tyl-H2, (**4**) Tyl-U, (**5**) Tyl=Tyr, (**6**) Tyl-Tyr, and (**7**) Tyl-Car to compete with radiolabeled erythromycin for binding to *D. radiodurans* 70S ribosomes was determined. The binding of erythromycin in the absence of competing ligand was assigned as 100%.

(B) Quantification of the fluorescence of GFP produced in an *E. coli* in vitro transcription-translation assay in the presence or absence of tylosin, (**1**) Tyl-H2, (**4**) Tyl-U, (**5**) Tyl=Tyr, (**6**) Tyl-Tyr, and (**7**) Tyl-Car. The fluorescence of GFP in the absence of antibiotic was assigned as 100%.

(C) Model based on Tyl-A2 for the binding site of (**7**) Tyl-Car (yellow) on the *D. radiodurans* 50S subunit showing the stacking interaction between the carinitine sidechain of (**7**) Tyl-Car and the base of A2062 of the 23S rRNA.

(D) The ability of tylosin, desmycosin (Des), OMT, (**8**) Tyl-Phe, (**9**) Des-Phe, and (**10**) OMT-Phe to compete with radiolabeled erythromycin for binding to *D. radiodurans* 70S ribosomes was determined. The binding of erythromycin in the absence of competing ligand was assigned as 100%.

(E) Quantification of the fluorescence of GFP produced in an *E. coli* in vitro transcription-translation assay in the presence or absence of tylosin, desmycosin (Des), OMT, (**8**) Tyl-Phe, (**9**) Des-Phe, and (**10**) OMT-Phe. The fluorescence of GFP in the absence of antibiotic was assigned as 100%.

(F) Model based on (**2**) Tyl-A2 for the binding site of (**8**) Tyl-Phe (purple) on the *D. radiodurans* 50S subunit showing the stacking interaction between the linker of (**8**) Tyl-Phe and the base of A2062, as well as a between the phenylalanine aromatic residue and the base of C2586 of the 23S rRNA.

a nonpolar phenylalanine (Phe), while extending the linker, but maintaining its overall flexibility. Binding studies indicate that this compound, (**8**) Tyl-Phe, improved the ribosome binding affinity (K_d, 3.6 nM) compared to (**1**) Tyl-H2 (Figure 4D; Table S1). Consistently, (**8**) Tyl-Phe was found to be a very potent inhibitor of translation (Figure 4E), performing slightly better than tylosin but significantly better than (**2**) Tyl-A2 and (**1**) Tyl-H2 (Table S1). The Phe side chain may stabilize the binding of (**8**) Tyl-Phe by establishing additional stacking interactions with 23S rRNA nucleotides (Figure 4F). However, the improved ribosome binding affinity cannot be the sole explanation for the increased translational inhibitory activity relative to tylosin, because (**8**) Tyl-Phe was significantly less effective compared to tylosin at competing erythromycin from the ribosome (Figure 4D).

We also synthesized (**9**) Des-Phe and (**10**) OMT-Phe, where the Phe-containing linker side chain was attached to the C20 position of desmycosin and OMT, respectively (Figure 1). OMT is a precursor of tylosin, which lacks both the C5 mycarose and the C23 mycinose (Figure 1). Our erythromycin competition studies indicate that both (**9**) Des-Phe and (**10**) OMT-Phe were worse competitors than their respective parent compounds (Figure 4D). The order of affinities of (**8**) Tyl-Phe > (**9**) Des-Phe > (**10**) OMT-Phe is the same as for tylosin > desmycosin > OMT, and correlates with the predicted surface areas that these compounds bury on the ribosome; that is, more surface area buried equals higher binding affinity (Hansen et al., 2002). However, that each derivative had a lower binding affinity than the parent compound emphasizes again the important influence that the C6-ethyl aldehyde and presumably the carbinolamine

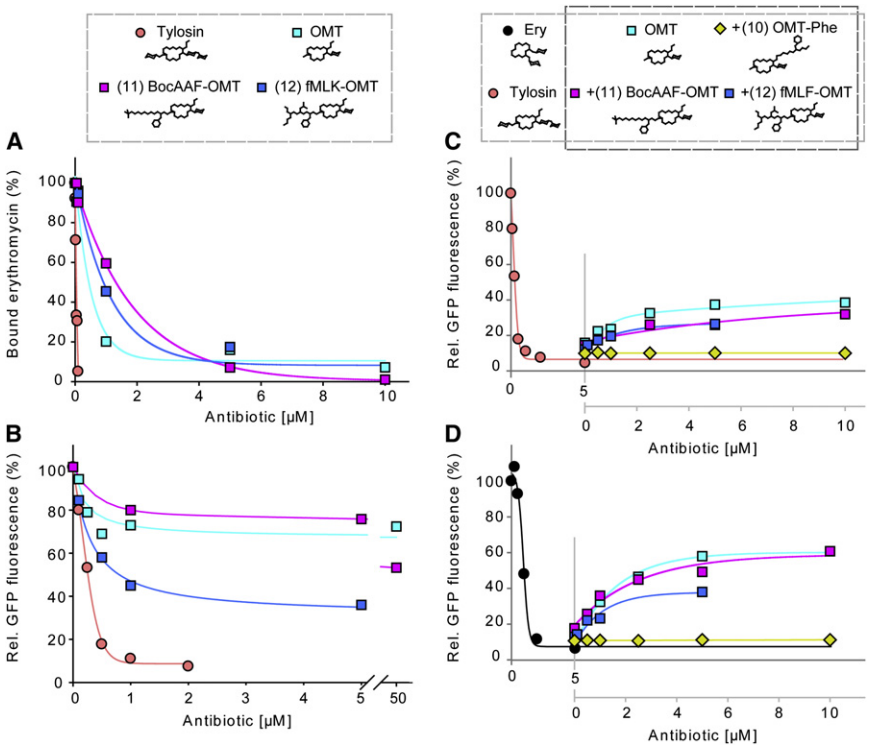

Figure 5. Protective Effects of OMT Compounds

(A) The ability of tylosin, OMT, (**11**) BocAAF-OMT, and (**12**) fMLF-OMT to compete with radiolabeled erythromycin for binding to *D. radiodurans* 70S ribosomes was determined. The binding of erythromycin in the absence of competing ligand was assigned as 100%.

(B) Quantification of the fluorescence of GFP produced in an *E. coli* in vitro transcription-translation assay in the presence or absence of tylosin, OMT, (**11**) BocAAF-OMT, and (**12**) fMLF-OMT. The fluorescence of GFP in the absence of antibiotic was assigned as 100%.

(C) Quantification of the fluorescence of GFP produced in an *E. coli* in vitro transcription-translation assay in the presence of increasing concentrations (upper *x*-axis) of erythromycin (Ery) to 5 μM, then with additional presence of increasing concentrations (lower *x*-axis) of OMT (cyan), (**11**) BocAAF-OMT (magenta), (**12**) fMLF-OMT (blue), or (**10**) OMT-Phe (yellow).

(D) Quantification of the fluorescence of GFP produced in an *E. coli* in vitro transcription-translation assay in the presence of increasing concentrations (upper *x*-axis) of tylosin (Ery) to 5 μM, then with additional presence of increasing concentrations (lower *x*-axis) of OMT (cyan), (**11**) BocAAF-OMT (magenta), (**12**) fMLF-OMT (blue), or (**10**) OMT-Phe (yellow).

bond has on stabilizing the C6-ethyl aldehyde–containing macrolides on the ribosome.

In the translation system, (**9**) Des-Phe and (**10**) OMT-Phe, like (**8**) Tyl-Phe, were more potent inhibitors than would have been expected on the basis of their K_d values. (**9**) Des-Phe and (**10**) OMT-Phe had IC_{50} values (0.1 μM and 0.3 μM, respectively) similar to that of tylosin (0.25 μM) (Figure 4E; Table S1), thus indicating that the presence of the peptide and its interaction with the tunnel can compensate for loss in binding affinity resulting from disruption of the covalent linkage with the ribosome. In contrast, we found unexpectedly that desmycosin and OMT were very poor inhibitors of translation. Even with high concentrations of antibiotic (50–100 μM), desmycosin never inhibited translation by more than 50% (Figure 3B), and OMT had little or no significant inhibitory effect (Figure 4E). This finding was surprising because (1) both OMT and desmycosin bound efficiently to an empty ribosome (Figure 4D), with K_d values of 3 nM and 0.3 nM, respectively (Table S1), similar to that previously reported (Karahalios et al., 2006) and that is 5- and 50-fold better than that of erythromycin (K_d, 15 nM) (Karahalios et al., 2006); and (2) both OMT and desmycosin have potent antimicrobial activity (data not shown). Indeed, OMT and desmycosin are known to have MIC values similar to tylosin for a number of gram-positive bacterial strains (e.g., *Streptococcus pyogenes*, *Staphlococcus aureus*, and *Enterococcus faecalis*) (Fu et al., 2006; Kirst et al., 1988; Mutak et al., 2004).

Protective Effects of Peptide-OMT Precursor Compounds Against Translation Inhibition

To investigate the differential effects of OMT in more detail, we synthesized a series of peptide-OMT compounds, where BocAlaAlaPhe and fMetLeuPhe peptides were attached to C14(C23) of OMT to generate (**11**) BocAAF-OMT and (**12**) fMLF-OMT derivatives, respectively. These compounds still retain a C5 sugar and the C6 ethyl aldehyde, and the placement of the peptide side chain on the C14(C23) position of the lactone ring orients it such that it would penetrate deeper into the ribosomal tunnel. Like OMT, both (**11**) BocAAF-OMT and (**12**) fMLF-OMT were excellent competitors of erythromycin, although the presence of the peptide did not enhance the affinity of the derivative for the ribosome (Figure 5A). In contrast, the presence of the peptide improved the inhibitory effect of the OMT derivatives, particularly, (**12**) fMLF-OMT, which inhibited the in vitro translation reaction by 50% at ~1 μM (Figure 5B).

Because OMT and some of the derivatives were shown to bind efficiently to an empty ribosome, but were poor inhibitors in the translation assay, we decided to test whether the compounds could relieve the translation inhibition effect that results from other more effective macrolide antibiotics, such as tylosin and erythromycin. Figure 5C shows that, at 5 μM erythromycin, the translation of GFP is totally abolished, whereas when OMT, (**11**) BocAAF-OMT, or (**12**) fMLF-OMT are additionally titrated into the reaction, the inhibition of translation was gradually alleviated. As a control, (**10**) OMT-Phe, which was shown itself to be a potent inhibitor (Figure 4E), could not relieve the inhibitory effect due to erythromycin (Figure 5C). Indeed, the extent of relief appeared to correlate inversely with the innate inhibitory activity of the compound; for example, OMT and (**11**) BocAAF-OMT, which were the poorest inhibitors, yielded the strongest relief (up to 40% with 5 μM—that is, equimolar concentration to erythromycin), whereas (**12**) fMLF-OMT, which was a slightly better inhibitor, only restored translation by up to 20% at 5 μM final

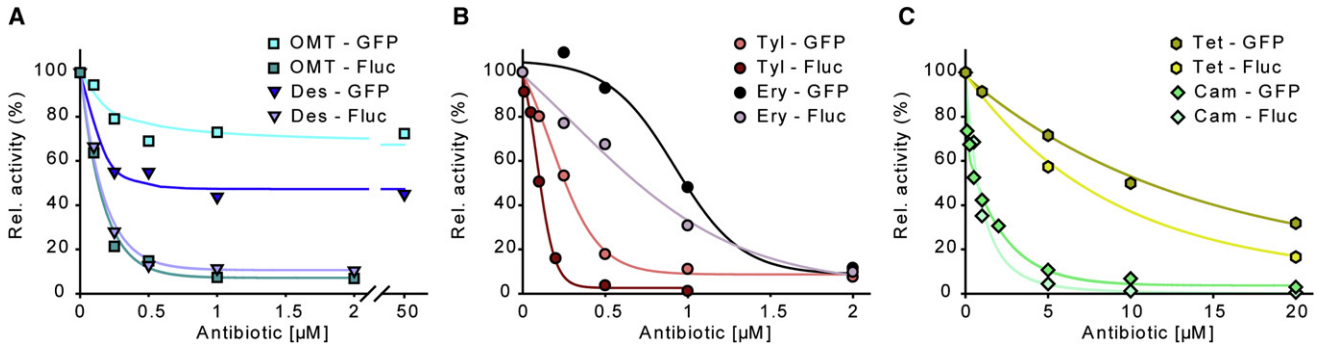

Figure 6. Polypeptide Chain-Dependency of Macrolide Antibiotics

(A) Comparison of the effect of desmycosin (Des) and OMT on the in vitro transcription-translation of green fluorescent protein (GFP) and firefly luciferase (Fluc).

(B) Comparison of the effect of tylosin (Tyl) and erythromycin (Ery) on the in vitro transcription-translation of GFP and Fluc.

(C) Comparison of the effect of chloramphenicol (Cam) and tetracycline (Tet) on the in vitro transcription-translation of GFP and Fluc. In (A)–(C), the fluorescence of GFP or luminescence of Fluc in the absence of antibiotic was assigned as 100%.

concentration (Figure 5C). This latter result was slightly surprising, since at 5 μM of (**12**) fMLF-OMT, the drug itself reduces translation by 60% (to 40%). Similar results were observed when 5 μM tylosin was used instead of erythromycin; however, higher excesses of OMT and the derivatives were required to obtain the equivalent inhibitory relief that was observed with erythromycin (Figure 5D). For example, 10 μM (2× tylosin concentration) of OMT produced only ~30% relief (Figure 5D). This trend is consistent with the higher affinity and IC_{50} of tylosin over erythromycin (Table S1) and thus supports the idea that the relief is due to direct competition between the OMT/OMT-derivative and the inhibitory compound (tylosin or erythromycin). Additional evidence includes the observations that (1) OMT/OMT-derivatives could not relieve the translation inhibition resulting from nonmacrolide antibiotics, such as tetracycline or thiostrepton (data not shown), and (2) compounds that were very poor competitors with erythromycin, such as (**1**) Tyl-H2 (Figure 3A), produced very low inhibition relief with extremely high excesses of compound—for example, 25 μM (5× excess) (**1**) Tyl-H2 produced 4% relief for 5 μM tylosin (data not shown).

Macrolide Antibiotics Exhibit Polypeptide-Specific Inhibitory Effects

Because of the inconsistency between the potent antimicrobial activity of OMT and the poor inhibitory activity in the in vitro translation assay, we decided to test whether OMT displayed some template-specific effects. To do this, we substituted the GFP template with firefly luciferase (Fluc) and monitored translation of Fluc using luminescence. Figure 6A shows that OMT is an excellent inhibitor of translation of Fluc, with an IC_{50} of 0.15 μM, similar to that observed for the inhibition of GFP synthesis by tylosin (0.25 μM). Similarly, we found that Des, which we had shown to be a poor inhibitor of GFP (Figure 3C), was a potent inhibitor of Fluc synthesis (Figure 6A). Less dramatic differences were observed when comparing the effect of tylosin and erythromycin on GFP and Fluc synthesis (Figure 6B). The effect of tylosin on GFP and Fluc synthesis was similar, whereas the corresponding values for erythromycin were 1 μM (GFP) and 0.75 μM (Fluc) (Table S1). We believe that this template dependency in inhibition is specific for the macrolide class of antibiotics, because we do not find such distinct inhibitory effects when examining the inhibition of other antibiotic classes, such as the tetracyclines or phenylpropanoids (i.e., chloramphenicol) (Figure 6C). Tetracycline inhibits GFP synthesis with an IC_{50} of 11 μM and Fluc with an IC_{50} of 7 μM, and chloramphenicol inhibits GFP and Fluc with the same IC_{50} of ~1 μM (Figure 6C).

DISCUSSION

The surface of the exit tunnel is largely hydrophilic and has no patches of hydrophobic surface large enough to form a significant binding site for hydrophobic sequences in nascent polypeptide chains (Nissen et al., 2000). Although this general "nonstick" characteristic of the exit tunnel may hold for the majority of polypeptides being synthesized by the ribosome, growing evidence indicates that particular nascent chain sequences interact with the ribosomal tunnel during their egression (Becker et al., 2009; Bhushan et al., 2010; Cruz-Vera et al., 2005; Cruz-Vera and Yanofsky, 2008; Gong and Yanofsky, 2002; Kosolapov and Deutsch, 2009; Lawrence et al., 2008; Lu and Deutsch, 2005a, 2005b, 2008; Nakatogawa and Ito, 2002; Seidelt et al., 2009; Tenson and Ehrenberg, 2002; Vazquez-Laslop et al., 2008; Woolhead et al., 2004). Here, we have utilized macrolide antibiotics to direct amino acid and peptide sequences to bind and interact with the ribosomal tunnel. Our results indicate that specific amino acid and peptide sequences can indeed establish distinct interactions with components of the ribosomal tunnel, such as stacking interactions between the backbone and aromatic moieties with nucleotide A2062 of the 23S rRNA. A2062 is a universally conserved nucleotide that appears to adopt different conformations within the ribosomal tunnel dependent upon the functional state of the ribosome. In the crystal structure of the apo *Haloarcula marismortui* 50S subunit, A2062 lies flat against the tunnel wall, whereas when P-site ligands are bound A2062 shifts position to extend into the lumen of the ribosomal tunnel (Figure 2B). It appears that A2062 also establishes interaction with the nascent polypeptide chains, as observed by cryo-EM of stalled translating ribosomes (Bhushan et al., 2010; Seidelt et al., 2009). Mutations of A2062 relieve the translational arrest resulting during synthesis of the ErmC leader peptide,

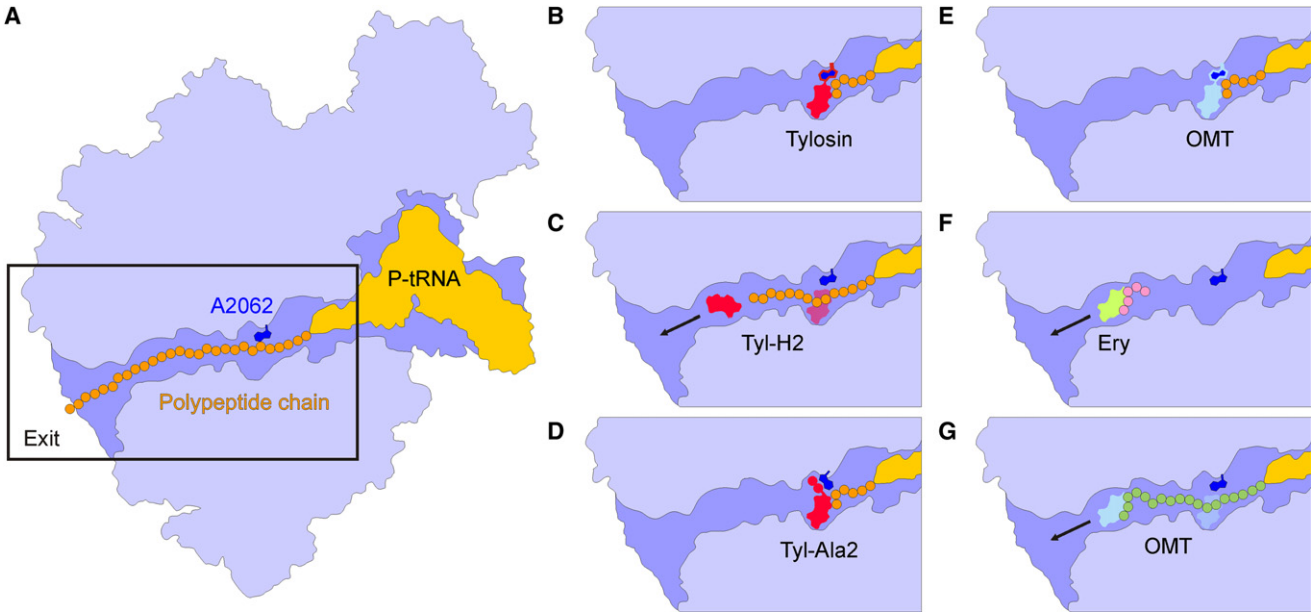

Figure 7. Factors Influencing Macrolide Inhibition

(A) Schematic view of a transverse section through the large ribosomal subunit revealing a P-site tRNA (yellow) attached to a polypeptide chain (orange) in the tunnel exit. The nucleotide A2062 (blue) has been proposed to interact with some polypeptide chains (Ramu et al., 2009; Vazquez-Laslop et al., 2008).

(B) Tylosin (red) binds within the tunnel where it forms a covalent bond with A2062 of the 23S rRNA and allows only translation of short peptides.

(C) Reducing the C6 ethylaldehyde of tylosin to produce (**1**) Tyl-H2 prevents the covalent interaction with A2062, reducing the binding affinity and allowing translation in the presence of the drug.

(D) Addition of amino acids or peptides to the C20 position prevents the covalent interaction with A2062, but establishes new compensatory interaction with the tunnel that increases the binding affinity and thus allows only translation of short peptides.

(E) OMT (cyan) binds within the tunnel where it forms a covalent bond with A2062 of the 23S rRNA and allows only translation of short peptides of the Fluc protein.

(F) Translation of short pentapeptide sequences confers resistance to macrolide antibiotics, such as erythromycin (Tenson et al., 1996). The peptide is thought to interact with the drug and remove it from the binding site when the peptide is released from the tRNA (Tenson and Mankin, 2001).

(G) Translation of GFP is not inhibited by OMT (cyan) either because the polypeptide chain removes the drug from its binding site or can pass the drug undisturbed.

suggesting that this nucleotide might be involved in monitoring the nascent chain as it passes through the tunnel (Figure 7A) (Vazquez-Laslop et al., 2008).

A2062 is also involved in the interaction of 16-membered macrolides, such as tylosin, with the ribosome because it forms a covalent bond with the drug. Here we show that reducing the C6-ethyl aldehyde of tylosin (Tyl-H2), which abolishes the potential to form a covalent linkage with the N6 of A2062, dramatically reduces the K_d value by >100-fold (Table S1). The corresponding loss in effectiveness of this antibiotic in translation inhibition is seen by a reduction in IC_{50} by >10-fold (Table S1), suggesting that the nascent polypeptide chain can now expel the drug from the ribosome (Figure 7C). It should be noted, however, that the presence of a C6-ethyl aldehyde is not strictly necessary for efficient binding and potent inhibitory activity because erythromycin has a C6-hydroxyl and thus cannot and does not form the carbinolamine bond (Tu et al., 2005). The differences in orientation (Hansen et al., 2002; Tu et al., 2005; Wilson et al., 2005) and kinetics (Petropoulos et al., 2009) of binding between 14-membered macrolides, such as erythromycin, and 16-membered macrolides, such as tylosin, seems to obviate the C6-ethyl aldehyde in the former case. It would be interesting in the future to analyze the characteristics of C6-ethyl aldehyde containing 14-membered macrolides, with respect to binding modes, kinetics, and formation of the carbinolamine interaction with A2062. Nevertheless, we could show that the loss of the covalent bond can be compensated for by addition of amino acid or peptide side chains to the C6(C23) position of the drug (Figure 7D). On the basis of the observation that (**2**) Tyl-A2 stacks upon the nucleobase of A2062 (Figures 3E and 7D), a series of compounds was designed to explore different modes of interactions with this region of the ribosome, culminating in a series of compounds—(**6**) Tyl-Tyr, (**7**) Tyl-Car, (**8**) Tyl-Phe, (**9**) Des-Phe, and (**10**) OMT-Phe—that were similar or better inhibitors of translation compared to tylosin (Figure 4; Table S1). These results also demonstrate the potential to use the ribosome antibiotic structures as a basis for rational design of novel derivatives of antimicrobial agents.

One observation with respect to many of the macrolide-peptide derivatives is the lack of correlation between the K_d and IC_{50} values, namely that all of the macrolide-peptide derivatives are less effective at competing erythromycin from the ribosome than are tylosin, but are relatively better inhibitors of translation. This suggests that the binding affinity per se does not solely determine the effectiveness of the compound and that the C20-side chains contribute an additional factor, perhaps by sterically blocking the path of the nascent polypeptide chain (Figure 7D). The most dramatic example of this is seen for

OMT and (**10**) OMT-Phe, because OMT has a K_d value ~9× lower than that of (**10**) OMT-Phe (Table S1), yet (**10**) OMT-Phe is a vastly superior inhibitor of GFP synthesis (Figure 4E). The ability of OMT and the peptide-OMT derivatives, (**11**) BocAAF-OMT and (**12**) fMLF-OMT to restore translation in the presence of inhibitory concentrations of erythromycin or tylosin (Figures 5C and 5D) is consistent with the binding data (Figures 4D and 5A), supporting the conclusion that these compounds do bind to the ribosome, and thus are likely to reverse the effect of erythromycin and tylosin by competing the drugs from their binding site in tunnel.

The lack of effect of OMT on GFP synthesis (Figures 5E and 6A) was surprising because OMT is known to be a potent antimicrobial agent that targets the translation machinery (Fu et al., 2006; Kirst et al., 1988; Mutak et al., 2004). This finding prompted us to test the effect of macrolides on translation of Fluc, which we could monitor using luminescence. OMT was found to be a potent inhibitor of Fluc synthesis (Figure 7E), as was tylosin (Figure 6A). Similarly, we found differential effects for desmycosin, which was a poor inhibitor of GFP but an excellent inhibitor of Fluc synthesis (Figure 6A). In contrast, few significant differences were observed between the inhibition of GFP and Fluc synthesis by other macrolides, such as tylosin (Figure 6B), erythromycin, (Figure 6C), nor for other classes of antibiotics, such as chloramphenicols and tetracyclines (Figure 6C). We also generated chimeric Fluc-GFP templates where the first 5–15 amino acids of Fluc were placed at the N terminus of GFP and vice versa. Unfortunately, the efficiency of translation of these proteins appeared to be dramatically affected, such that the interpretation of the results was inconclusive (data not shown).

Collectively, the data suggest that the sequence of the nascent chain may influence the inhibitory ability of particular macrolide antibiotics. Precedents for this include the observation that translation of specific pentapeptides can confer resistance to macrolide antibiotics by chasing the drug from the ribosome (Figure 7F). Distinct pentapeptides sequences are specific for particular macrolide or ketolide members, leading to the proposal of a direct interaction between the nascent chain and the drug in the ribosomal tunnel (Lovmar et al., 2006; Tenson et al., 1996; Tenson and Mankin, 2001; Tenson et al., 1997; Tripathi et al., 1998; Vimberg et al., 2004). By analogy, we propose that the GFP nascent polypeptide chain establishes specific interactions with OMT, leading to its removal from the ribosome (Figure 7G).

Because macrolide antibiotics cannot bind to and inhibit translating ribosomes (Contreras and Vazquez, 1977; Tai et al., 1974), we do not believe that the differential inhibitory effects of OMT on GFP and Fluc synthesis result from the ability of the GFP, but not Fluc, nascent polypeptide chain to pass the drug in the exit tunnel, but we cannot totally exclude this possibility. Macrolide antibiotics have been shown to allow synthesis of up to six to eight amino acids before peptidyl-tRNA drop-off occurs (Tenson et al., 2003). This may hint that the N-terminal six to eight residues of translating nascent chains, in this case GFP, interacts with drug (OMT) and removes it from the tunnel by continued translation of the nascent chain (Figure 7G) as suggested previously (Mankin, 2008), in contrast to drug removal via peptidyl-tRNA hydrolysis, as occurs in the case of the macrolide-resistance peptides (Figure 7F) (Tenson and Ehrenberg, 2002).

The proposed model suggests that the translation of a particular subset of proteins in vivo may not be inhibited by macrolide antibiotics, which could potentially provide the cell an additional regulatory mechanism, for example, to up-regulate relevant resistance genes. Future works needs to address the ubiquity of this "translating nascent chain-mediated macrolide resistance" and to determine whether specific consensus sequences exist for distinct macrolides.

EXPERIMENTAL PROCEDURES

Synthesis of Peptide Derivatives of Macrolides

(**1**) Tyl-H2 was prepared by reduction of Tyl with sodium borohydride (Kirst et al., 1988). (**2**) Tyl-A2 and (**3**) Des-A2 were synthesized as described elsewhere (Sumbatyan et al., 2003). (**8**) Tyl-Phe, (**9**) Des-Phe, and (**10**) OMT-Phe were prepared by analogy with (**2**) Tyl-A2 and (**3**) Des-A2 (Sumbatyan et al., 2003) by the condensation of 2-aminooxyacetylphenylalanyl ethyl ester with Tyl (Des or OMT) in 0.4 M Na-acetate buffer (pH 4.7) at 50°C (Sumbatyan et al., 2010). (**4**) Tyl-U and (**5**) Tyl = Tyr were prepared by coupling of Tyl with 3-(uracyl-1-yl)alanine (or tyrosine) in methanol in the presence of sodium methylate at room temperature. (**5**) Tyl = Tyr was reduced with sodium borohydride to give (**6**) Tyl-Tyr (Sumbatyan et al., 2010). The compounds were purified by the column chromatography on silica gel, and their homogeneity and structure were confirmed by TLC, HPLC, NMR, and mass spectra. BocAAF-OMT and fMLF-OMT were synthesized as described elsewhere (Korshunova et al., 2007). (**7**) Tyl-Car was synthesized starting from tylosin (24 mg, 0.026 mmol, 1 eq.) and carnitine hydrazide (Oka et al., 1963) (8 mg, 0.045 mmol, 1.7 eq.), which were dissolved in Na-acetate buffer (pH 4.7) (1.5 ml), and the mixture was stirred for 12 hr at 50°C. The crude product was extracted with chloroform and purified by silica gel column chromatography in chloroform-methanol (3:1, v/v) system to give (**7**) Tyl-Car as white crystals: the yield, 42% (11.1 mg, 0.011 mmol); TLC: R_f ($CHCl_3$ - CH_3OH, 3:1) 0;7, R_f ($CHCl_3$ - CH_3OH – CH_3COOH, 6:1:0.1) 0;25, R_f ($CHCl_3$ - CH_3OH, 6:1) 0;28, HPLC: t_R = 19.7 min (gradient of CH_3CN in 0,1% CF_3COOH 0%–60%); MALDI MS: m/z calculated. for $C_{53}H_{93}N_4O_{18}$ 1073.7; found 1070.6; NMR ^1H (600 MHz, 303K, DMSO): 0.86 (3H, t, H17), 0.94 (3H, d, H18), 1.08 (3H, d, H5"CH_3), 1.15 (3H, s, H3"CH_3), 1.23 (3H, d, H21), 1.25 (3H, d, H5′CH_3), 1.28 (3H, d, H5′"CH_3), 1.58 (1H, m, H16), 1.65 (2H, m, H4, H2"), 1.80 (3H, s, H22), 1.82 (4H, m, H7, H16, H2," $H^{\alpha\ Car}$), 1.90 (3H, m, H2, H7, H16), 1.95 (1H, m, H2), 2.48 (6H, 1H, s, m, $N(CH_3)_3$, H3′), 2.77 (2H, m, H6, H19), 2.88 (1H, m, H14), 2.98 (1H, dd, H2′"), 3.13 (m, 4H, H8, H4′, H5′), 3.38 (1H, m, H2′), 3.39 (9H, s, $N^+(CH_3)_3^{Car}$), 3.41 (2H, m, H5," H3), 3.44 (3H, s, H2′"OCH_3), 3.50 (3H, s, H3′"OCH_3), 3.52 (3H, m, $H^{\gamma\ Car}$, H23), 3.61 (3H, m, H3′", H5, H5′"), 3.80 (1H, m, H23), 4.12 (3H, m, H1′, H4," $H^{\beta\ Car}$), 4.38 (1H, m, H4′"), 4.47 (1H, d, H1′"), 4.95 (3H, m, H15, H1," NH^{Car}), 5.82 (1H, d, H13), 6.49 (1H, d, H10), 7.10 (1H, d, H11), 8.16 (1H, s, H20).

In Vitro Transcription-Translation Assay

All coupled transcription-translation experiments were performed using an *E. coli* lysate–based system in the presence and absence of antibiotics, as described elsewhere (Dinos et al., 2004; Starosta et al., 2009; Szaflarski et al., 2008). Two microliters of each reaction was diluted with 50 μL of buffer A (10 mM HEPES/KOH [pH 7.8], 10 mM $MgCl_2$, 60 mM NH_4Cl, and 4 mM β-mercaptoethanol), mixed, and then transferred into black 96-well chimney flat bottom microtiter plates. The GFP fluorescence was either on a Tecan Infinite® M1000 with an excitation wavelength of 395 nm and emission 509 nm, or measured at 520 nm (filter cutoff) with a Typhoon Scanner 9400 (Amersham Bioscience) using a Typhoon blue laser module (excited at 488 nm). Images were then quantified using ImageQuantTL (GE Healthcare) and were represented graphical using SigmaPlot (Systat Software, Inc.). Synthesis of firefly luciferase (Fluc) was performed as described above for GFP, but using pIVEX-2.3MCS with Fluc cloned into the NdeI and SacI restriction sites as a template. After incubation at 30°C with shaking for 4–5 hr, 2 μL of each reaction was added directly to white 96-well chimney flat bottom microtiter plates, after which 50 μL of luminol substrate (Promega) was quickly added, shaken for 3 s, and the luminescence was immediately detected using

a Tecan Infinite® M1000. All measurements were repeated in triplicate and had a standard deviation of less than 10%.

Binding Assay

Binding of all compounds to empty ribosomes was examined using a competition assay with radiolabeled [^{14}C]Erythromycin (Perkin Elmer), as described elsewhere (Karahalios et al., 2006; Petropoulos et al., 2009). Briefly, all reactions contained 0.25 μM *D. radiodurans* 70S ribosomes and 1.25 μM [^{14}C]erythromycin in binding buffer (10 mM HEPES/KOH [pH 7.8], 30 mM $MgCl_2$, 150 mM NH_4Cl, and 6 mM β-mercaptoethanol), which equated with 60% binding from the saturation curve (data not shown). The saturation curve indicated that 80% of ribosomes were active (data not shown). To measure the apparent K_d value for each of the compound, reactions were performed in the absence or presence of increasing concentrations of the competing compounds. After incubation at room temperature for 2 hr, reactions were passed through nitrocellulose filters, type HA, 0.45 μm pore size (Millipore). Filters were washed three times with binding buffer and then scintillation counted in the presence of Filtersafe (Zinsser Analytic) scintillant. All measurements were repeated in duplicate and had a standard deviation of 5%–10%.

Modeling and Figure Preparation

All chemical structures were drawn with ChemSketch and then were modified with Adobe Illustrator. Small molecule structures for macrolide-peptide derivatives were generated using ChemSketch. The lactone rings were then replaced with the lactone ring from *D. radiodurans* 50S subunit in complex with (**2**) Tyl-A2 (Wilson et al., 2005), and the derivative sidechains were modeled on the basis of the position of the Ala-Ala sidechain of (**2**) Tyl-A2. The models of the macrolide-peptide compounds in complex with the large subunit were then minimized using CNS (Brünger et al., 1998). All 3D structural figures were produced using PyMol (http://www.pymol.org).

SUPPLEMENTAL INFORMATION

Supplemental information includes one table and can be found with this article online at doi:10.1016/j.chembiol.2010.04.008.

ACKNOWLEDGMENTS

We thank Shura Mankin and Roland Beckmann for helpful discussions, and the Beckmann laboratory for generous support and creating a stimulating work environment. This study was financed by the Deutsche Forschungsgemeinschaft (grant WI3285/1-1 to D.N.W.) and the Russian Foundation for Basic Research (grant 07-04-00902a to G.A.K.). V.K. would like to acknowledge the FEBS Fellowship Committee for granting her a Collaborative Experimental Scholarship for Central and Eastern Europe. A.A.B. would like to thank the Alexander von Humboldt Foundation for a very generous support.

Received: February 23, 2010
Revised: March 22, 2010
Accepted: April 2, 2010
Published: May 27, 2010

REFERENCES

Becker, T., Bhushan, S., Jarasch, A., Armache, J.P., Funes, S., Jossinet, F., Gumbart, J., Mielke, T., Berninghausen, O., Schulten, K., et al. (2009). Structure of monomeric yeast and mammalian Sec61 complexes interacting with the translating ribosome. Science *326*, 1369–1373.

Bhushan, S., Gartmann, M., Halic, M., Armache, J.P., Jarasch, A., Mielke, T., Berninghausen, O., Wilson, D.N., and Beckmann, R. (2010). α-helical nascent polypeptide chains visualized within distinct regions of the ribosomal exit tunnel. Nat. Struct. Mol. Biol. *17*, 313–317.

Brünger, A.T., Adams, P.D., Clore, G.M., DeLano, W.L., Gros, P., Grosse-Kunstleve, R.W., Jiang, J.S., Kuszewski, J., Nilges, M., Pannu, N.S., et al. (1998). Crystallography & NMR system: a new software suite for macromolecular structure determination. Acta Crystallogr. D Biol. Crystallogr. *54*, 905–921.

Contreras, A., and Vazquez, D. (1977). Cooperative and antagonistic interactions of peptidyl-tRNA and antibiotics with bacterial ribosomes. Eur. J. Biochem. *74*, 539–547.

Cruz-Vera, L.R., and Yanofsky, C. (2008). Conserved residues Asp16 and Pro24 of TnaC-tRNAPro participate in tryptophan induction of Tna operon expression. J. Bacteriol. *190*, 4791–4797.

Cruz-Vera, L.R., Rajagopal, S., Squires, C., and Yanofsky, C. (2005). Features of ribosome-peptidyl-tRNA interactions essential for tryptophan induction of tna operon expression. Mol. Cell *19*, 333–343.

Dinos, G., Wilson, D.N., Teraoka, Y., Szaflarski, W., Fucini, P., Kalpaxis, D., and Nierhaus, K.H. (2004). Dissecting the ribosomal inhibition mechanisms of edeine and pactamycin: the universally conserved residues G693 and C795 regulate P-site tRNA binding. Mol. Cell *13*, 113–124.

Fu, H., Marquez, S., Gu, X., Katz, L., and Myles, D.C. (2006). Synthesis and in vitro antibiotic activity of 16-membered 9-O-arylalkyloxime macrolides. Bioorg. Med. Chem. Lett. *16*, 1259–1266.

Gong, F., and Yanofsky, C. (2002). Instruction of translating ribosome by nascent peptide. Science *297*, 1864–1867.

Hansen, J.L., Ippolito, J.A., Ban, N., Nissen, P., Moore, P.B., and Steitz, T.A. (2002). The structures of four macrolide antibiotics bound to the large ribosomal subunit. Mol. Cell *10*, 117–128.

Karahalios, P., Kalpaxis, D.L., Fu, H., Katz, L., Wilson, D.N., and Dinos, G.P. (2006). On the mechanism of action of 9-O-arylalkyloxime derivatives of 6-O-mycaminosyltylonolide, a new class of 16-membered macrolide antibiotics. Mol. Pharmacol. *70*, 1271–1280.

Kirst, H.A., Toth, J.E., Debono, M., Willard, K.E., Truedell, B.A., Ott, J.L., Counter, F.T., Felty-Duckworth, A.M., and Pekarek, R.S. (1988). Synthesis and evaluation of tylosin-related macrolides modified at the aldehyde function: a new series of orally effective antibiotics. J. Med. Chem. *31*, 1631–1641.

Korshunova, G.A., Sumbatyan, N.V., Fedorova, N.V., Kuznetsova, I.V., Shishkina, A.V., and Bogdanov, A.A. (2007). Peptide derivatives of tylosin-related macrolides [in Russian]. Bioorg. Khim. *33*, 235–244.

Kosolapov, A., and Deutsch, C. (2009). Tertiary interactions within the ribosomal exit tunnel. Nat. Struct. Mol. Biol. *16*, 405–411.

Lawrence, M.G., Lindahl, L., and Zengel, J.M. (2008). Effects on translation pausing of alterations in protein and RNA components of the ribosome exit tunnel. J. Bacteriol. *190*, 5862–5869.

Lovmar, M., Nilsson, K., Vimberg, V., Tenson, T., Nervall, M., and Ehrenberg, M. (2006). The molecular mechanism of peptide-mediated erythromycin resistance. J. Biol. Chem. *281*, 6742–6750.

Lu, J., and Deutsch, C. (2005a). Folding zones inside the ribosomal exit tunnel. Nat. Struct. Mol. Biol. *12*, 1123–1129.

Lu, J., and Deutsch, C. (2005b). Secondary structure formation of a transmembrane segment in Kv channels. Biochemistry *44*, 8230–8243.

Lu, J., and Deutsch, C. (2008). Electrostatics in the ribosomal tunnel modulate chain elongation rates. J. Mol. Biol. *384*, 73–86.

Mankin, A.S. (2008). Macrolide myths. Curr. Opin. Microbiol. *11*, 414–421.

Mayford, M., and Weisblum, B. (1989). ermC leader peptide: amino acid sequence critical for induction by translational attenuation. J. Mol. Biol. *206*, 69–79.

Mutak, S., Marsic, N., Kramaric, M.D., and Pavlovic, D. (2004). Semisynthetic macrolide antibacterials derived from tylosin: synthesis and structure-activity relationships of novel desmycosin analogues. J. Med. Chem. *47*, 411–431.

Nakatogawa, H., and Ito, K. (2002). The ribosomal exit tunnel functions as a discriminating gate. Cell *108*, 629–636.

Narandja, A., Suskovic, B., Kelneric, Z., and Djokic, S. (1994). Structure-activity relationship among polyhydro derivatives of tylosin. J. Antibiot. (Tokyo) *47*, 581–587.

Nissen, P., Hansen, J., Ban, N., Moore, P.B., and Steitz, T.A. (2000). The structural basis of ribosome activity in peptide bond synthesis. Science *289*, 920–930.

Oka, Y., Yonemoto, H., and Yurugi, S. (1963). Carnitine derivatives. Takeda Kenkyusho Nenpo *22*, 13–18.

Omura, S., and Tishler, M. (1972). Relationship of structures and microbiological activities of the 16-membered macrolides. J. Med. Chem. *15*, 1011–1015.

Omura, S., Miyano, K., Matsubara, H., and Nakagawa, A. (1982). Novel dimeric derivatives of leucomycins and tylosin, sixteen-membered macrolides. J. Med. Chem. *25*, 271–275.

Petropoulos, A.D., Kouvela, E.C., Starosta, A.L., Wilson, D.N., Dinos, G.P., and Kalpaxis, D.L. (2009). Time-resolved binding of azithromycin to *Escherichia coli* ribosomes. J. Mol. Biol. *385*, 1179–1192.

Poehlsgaard, J., and Douthwaite, S. (2003). Macrolide antibiotic interaction and resistance on the bacterial ribosome. Curr. Opin. Investig. Drugs *4*, 140–148.

Poulsen, S.M., Kofoed, C., and Vester, B. (2000). Inhibition of the ribosomal peptidyl transferase reaction by the mycarose moiety of the antibiotics carbomycin, spiramycin and tylosin. J. Mol. Biol. *304*, 471–481.

Ramu, H., Mankin, A., and Vazquez-Laslop, N. (2009). Programmed drug-dependent ribosome stalling. Mol. Microbiol. *71*, 811–824.

Schlünzen, F., Zarivach, R., Harms, J., Bashan, A., Tocilj, A., Albrecht, R., Yonath, A., and Franceschi, F. (2001). Structural basis for the interaction of antibiotics with the peptidyl transferase centre in eubacteria. Nature *413*, 814–821.

Seidelt, B., Innis, C.A., Wilson, D.N., Gartmann, M., Armache, J.P., Villa, E., Trabuco, L.G., Becker, T., Mielke, T., Schulten, K., et al. (2009). Structural insight into nascent polypeptide chain-mediated translational stalling. Science *326*, 1412–1415.

Spahn, C.M.T., and Prescott, C.D. (1996). Throwing a spanner in the works: antibiotics and the translational apparatus. J. Mol. Med. *74*, 423–439.

Starosta, A.L., Qin, H., Mikolajka, A., Leung, G.Y., Schwinghammer, K., Nicolaou, K.C., Chen, D.Y., Cooperman, B.S., and Wilson, D.N. (2009). Identification of distinct thiopeptide-antibiotic precursor lead compounds using translation machinery assays. Chem. Biol. *16*, 1087–1096.

Sumbatyan, N.V., Korshunova, G.A., and Bogdanov, A.A. (2003). Peptide derivatives of antibiotics tylosin and desmycosin, protein synthesis inhibitors. Biochemistry (Mosc.) *68*, 1156–1158.

Sumbatyan, N.V., Kuznetsova, I.V., Karpenko, V.V., Federova, N.V., Chertkov, V.A., Korshunova, G.V., and Bogdanov, A.A. (2010). Amino acid and peptide derivatives of the tylosin family of antibiotics modified by aldehyde function. Russ. J. Bioorganic Chem. *36*, 245–256.

Szaflarski, W., Vesper, O., Teraoka, Y., Plitta, B., Wilson, D.N., and Nierhaus, K.H. (2008). New features of the ribosome and ribosomal inhibitors: non-enzymatic recycling, misreading and back-translocation. J. Mol. Biol. *380*, 193–205.

Tai, P.-C., Wallace, B.J., and Davis, B.D. (1974). Selective action of erythromycin on initiating ribosomes. Biochemistry *13*, 4653–4659.

Tenson, T., and Ehrenberg, M. (2002). Regulatory nascent peptides in the ribosomal tunnel. Cell *108*, 591–594.

Tenson, T., and Mankin, A. (2001). Short peptides conferring resistance to macrolide antibiotics. Peptides *22*, 1661–1668.

Tenson, T., Deblasio, A., and Mankin, A. (1996). A functional peptide encoded in the *Escherichia coli* 23S rRNA. Proc. Natl. Acad. Sci. USA *93*, 5641–5646.

Tenson, T., Xiong, L.Q., Kloss, P., and Mankin, A.S. (1997). Erythromycin resistance peptides selected from random peptide libraries. J. Biol. Chem. *272*, 17425–17430.

Tenson, T., Lovmar, M., and Ehrenberg, M. (2003). The mechanism of action of macrolides, lincosamides and streptogramin B reveals the nascent peptide exit path in the ribosome. J. Mol. Biol. *330*, 1005–1014.

Tripathi, S., Kloss, P.S., and Mankin, A.S. (1998). Ketolide resistance conferred by short peptides. J. Biol. Chem. *273*, 20073–20077.

Tu, D., Blaha, G., Moore, P., and Steitz, T. (2005). Structures of MLSBK antibiotics bound to mutated large ribosomal subunits provide a structural explanation for resistance. Cell *121*, 257–270.

Vazquez-Laslop, N., Thum, C., and Mankin, A.S. (2008). Molecular mechanism of drug-dependent ribosome stalling. Mol. Cell *30*, 190–202.

Vimberg, V., Xiong, L., Bailey, M., Tenson, T., and Mankin, A. (2004). Peptide-mediated macrolide resistance reveals possible specific interactions in the nascent peptide exit tunnel. Mol. Microbiol. *54*, 376–385.

Wilson, D.N. (2009). The A-Z of bacterial translation inhibitors. Crit. Rev. Biochem. Mol. Biol. *44*, 393–433.

Wilson, D.N., Harms, J.M., Nierhaus, K.H., Schlünzen, F., and Fucini, P. (2005). Species-specific antibiotic-ribosome interactions: Implications for drug development. Biol. Chem. *386*, 1239–1252.

Woolhead, C.A., McCormick, P.J., and Johnson, A.E. (2004). Nascent membrane and secretory proteins differ in FRET-detected folding far inside the ribosome and in their exposure to ribosomal proteins. Cell *116*, 725–736.

 ©2010 Elsevier Ltd All rights reserved